*ENGINEERING TRANSACTIONS* • *Engng. Trans.* • **65**, 3, 523–538, 2017
Polish Academy of Sciences • Institute of Fundamental Technological Research (IPPT PAN)
National Engineering School of Metz (ENIM) • Poznan University of Technology

## Research Paper

# Strength Analysis of Typical Koepe Pulley Constructions Applied in Mine Hoisting Installations

Stanisław WOLNY, Bogusław ŁADECKI

*AGH University of Science and Technology*
*Faculty of Mechanical Engineering and Robotics*
Al. Mickiewicza 30, 30-059 Kraków, Poland
e-mail: {stwolny, boglad}@agh.edu.pl

A large number of hoisting installations equipped with Koepe pulleys are presently operating in Polish mines. In many instances, cracks of fatigue character occur in those Koepe pulley constructions. Conducting periodic repairs in the areas of crack formations only temporarily fixes this issue. In order to eliminate this problem, this study aims at identifying the sources of fatigue crack formation and growth in Koepe pulleys. With this objective, the numerical models of the Koepe pulley construction were developed and analysed using the finite element method (FEM). The FEM analysis was preceded by the dynamic analysis of the hoisting installation during its normal work cycle. The results of these analyses – dynamic and strength – were verified by experiments on the real object by measuring forces and stresses in the selected areas of the pulley wheel. The obtained results provided the grounds for assessing the fatigue life and for introducing an improvement to the design of the considered Koepe pulley constructions.

**Key words:** Koepe pulley in hoisting installations, strength, material fatigue, experimental tests, non-destructive tests, FEM.

## 1. Introduction

Presently, Polish mining utilises a significant number of shaft hoists, in which operation period exceeds 30 years. These machines are usually either equipped with Koepe pulleys with U-shaped diaphragms joining the wheel side disks or with two circumferential rings stiffening the wheel mantle. Numerous cracks of fatigue character are observed in such wheels [1–3], and periodical repairs conducted on those wheels do not eliminate the sources of cracks reoccurring in the same areas of structure. Fast growing fatigue cracks and the necessity of frequent repairs essentially limit the safety and efficiency of hoisting installations. The results of non-destructive dynamic and strength analyses, verified by measuring the deformations on the actual objects are presented in this paper.

Our investigation aimed at explaining the sources of crack formations in Koepe pulleys and at proposing changes that will eliminate these sources.

## 2. Dynamic load acting on a Koepe Pulley under typical operating conditions

The actual loads acting on the pulley drum are obtained from the dynamic analysis of its operation throughout a typical duty cycle [4]. Since the tower-type winding installations with pulley blocks are now in widespread use in Polish collieries, this analysis will be thus solely confined to such type of hoisting installation, shown schematically in Fig. 1.

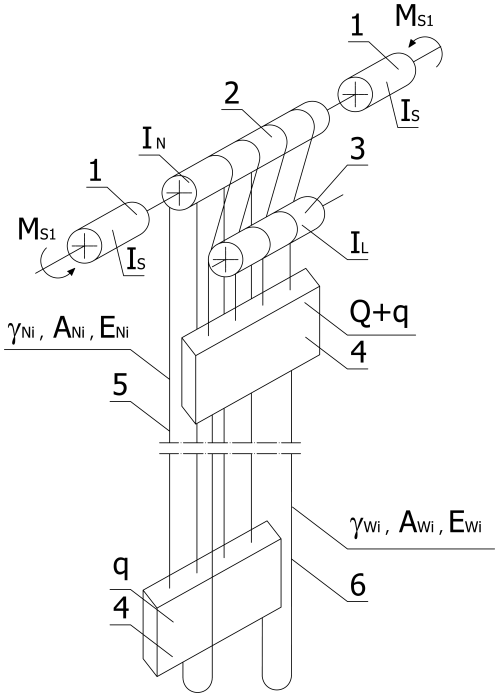


Fig. 1. Schematic diagram of hoisting installation: 1 – low speed DC motor, 2 – multi-rope pulley block with diameter $D$ and inertia moment $I_N$, 3 – baffle wheel assembly, 4 – skips (conveyance) with mass q and loading capacity $Q$, 5 – bundle of parallel hoisting ropes with density $\gamma_N$ and tensile rigidity $A_{Ni}E_{Ni}$, 6 – bundle of parallel balance ropes with density $\gamma_{Wi}$ and tensile rigidity $A_{Wi}E_{Wi}$.

The results of dynamic analyses in [4] and the measurements taken on a real object presented in [5, 6] provide the bases for deriving the analytical formulas to compute the maximal and minimal loads transmitted from the hoisting ropes onto the wheel in the winding gear.

The maximal loads are transmitted from the hoisting ropes onto the wheel at the instant when a full conveyance begins to be hoisted from the bottom level and are given as [4]

$$S_{\max} = S_{St}^{R} + \Delta S^{R}, \tag{2.1}$$

where $S_{St}^{R}$ – maximum static load transmitted from the rope onto the Koepe pulley in the start-up phase,

$$\Delta S^{R} = A_N E_N \frac{a_1}{a_N} \frac{8 l_N}{a_N} \left[1 - e^{-k}\right] \frac{1}{k},$$

$$k = \frac{A_N E_N}{M_2 a_N}, \qquad M_2 = Q + q, \tag{2.2}$$

$$\sum_{i=1}^{n} A_{Ni} E_{Ni} = A_N E_N,$$

$n$ – number of hoisting ropes, $a_1$ – acceleration in a start-up phase, $a_N$ – velocity of elastic wave propagation in hoisting ropes, $l_N$ – hoisting rope length at the instant when the full conveyance begins to move upward from the bottom level.

The minimum loads are transmitted from the hoisting ropes onto the drum at the instant when the full conveyance approaching the station begins a braking phase and are given as [5]

$$S_{\min} = S_{St}^{H} + \Delta S^{H}, \tag{2.3}$$

where $S_{St}^{H}$ – static load transmitted from the hoisting ropes onto the Koepe pulley at the instant when the full conveyance begins to brake when approaching the top level

$$\Delta S^{H} \equiv -A_N E_N \cdot \frac{a_2}{a_N} \cdot \frac{20.5 l^*}{a_N}, \tag{2.4}$$

$a_2$ – deceleration of braking in hoisting installation, $l^*$ – hoisting rope length measured from the Koepe pulley to the conveyance at the instant when the braking phase begins in the normal duty cycle.

Using dependencies (2.1) to (2.4) for the hoisting installation operating in one of the Polish mines [1] the maximum and minimum total force (load) values in hoisting ropes on both sides of the Koepe pulley were determined. These values are: $S_{\max} = 529.5$ kN and $S_{\min} = 441.1$ kN, respectively.

Assuming that all ropes have a uniform load, for further calculations the loads of an individual rope were taken as

$$S_{\max}^{(1)} = S_{\max}/n = 529.5/4 = 132.4 \text{ kN},$$

$$S_{\min}^{(1)} = S_{\min}/n = 441.5/4 = 110.3 \text{ kN},$$

where $n = 4$ – number of hoisting ropes.

## 3. Non-destructive tests of Koepe pulleys

In order to determine the ranges, character and intensity of fatigue failure occurrence in Koepe pulleys of the two considered designs: one with U-shaped diaphragms and the other with two circumferential rings reinforcing the mantle, both used in selected Polish mines, non-destructive testing was performed by means of the magnetic-powder and ultrasound methods. The performed investigations indicated the occurrence of numerous cracks. Examples of crack types for the pulley with 'U' diaphragms are shown in Fig. 2 [1, 2], and for the pulley with circumferential stiffening rings in Fig. 3 [3].

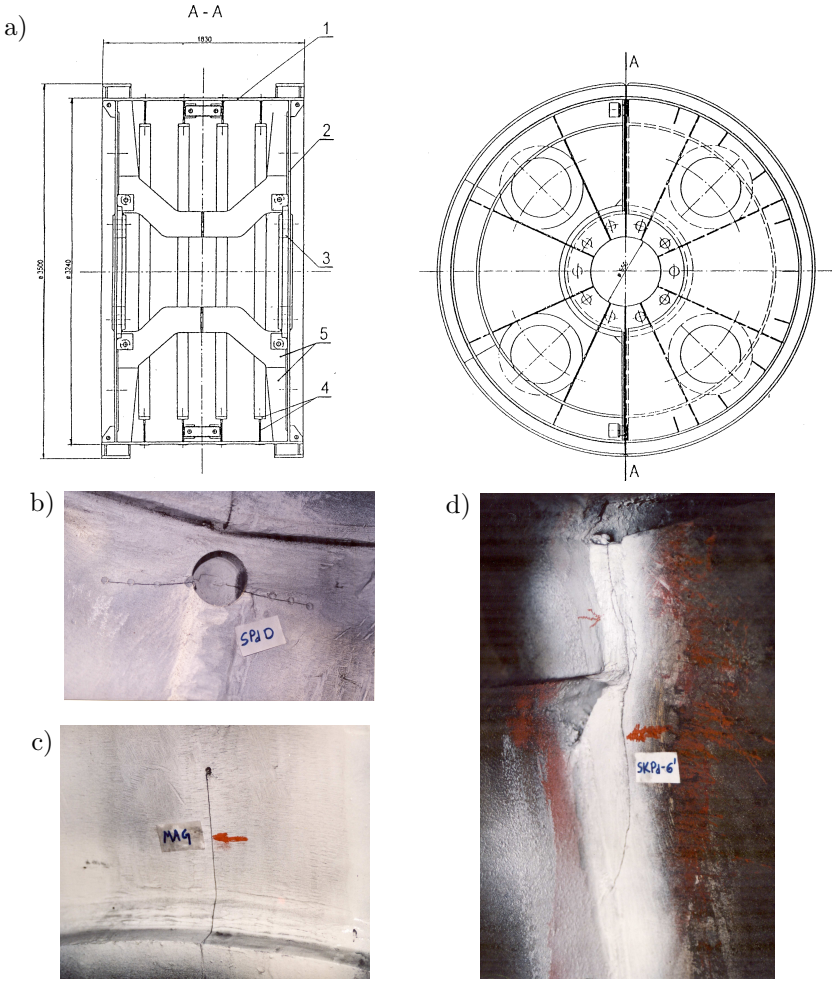


Fig. 2. a) Schematic presentation of the Koepe pulley with 'U' diaphragms: 1 – mantle, 2 – disk, 3 – hub, 4 – circumferential ring, 5 – diaphragm. Fatigue cracks within the side disk area: b) circumferential, and c) radial cracks. d) Crack in the area where the U' diaphragm joins with the side disk and hub [1].

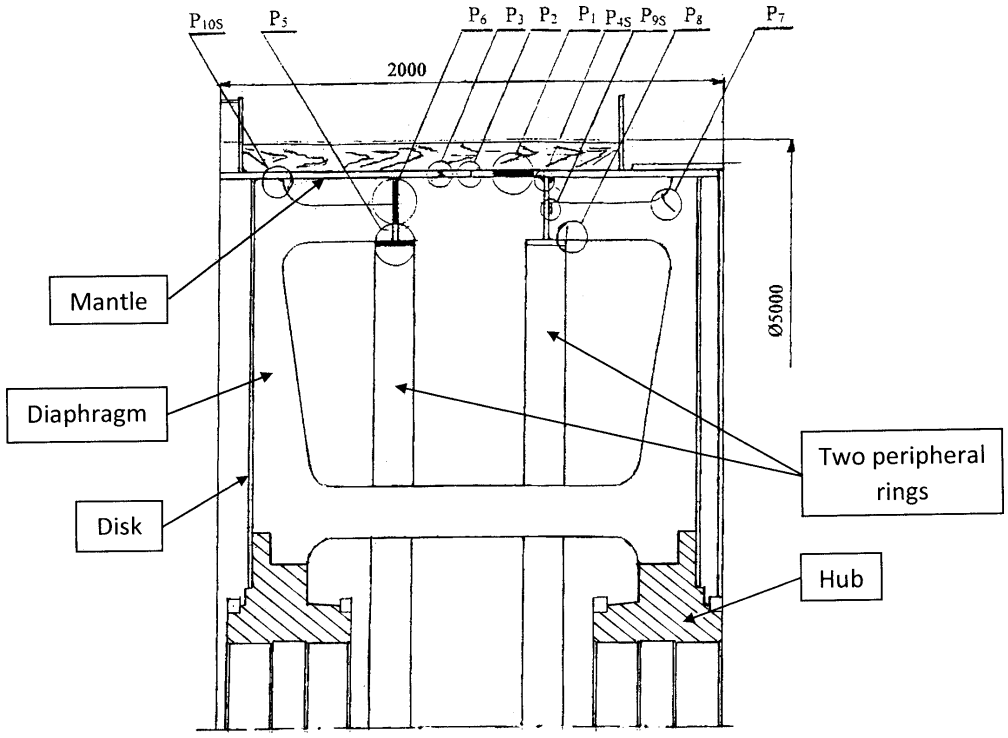


FIG. 3. Schematic diagram of the Koepe pulley with two peripheral reinforcing rings and the types of detected cracks [3].

Crack types detected on drums: $P_1(P_{1S})$ – cracking of the mantle material (butt weld) in the direction of the generating line, $P_2(P_{2S})$ – peripheral cracking of the mantle material (butt weld), $P_3(P_{3S})$ – transverse cracking of the mantle material (butt weld), $P_{4S}$ – peripheral cracking of fillet weld connecting the web of the peripheral rib with the mantle, $P_5(P_{5S})$ – cracking of the shelf (butt weld) of the peripheral rib, $P_6(P_{6S})$ – radial or skewed cracking of the web (butt weld of the web or the fillet weld of the web bit) of the peripheral ribs, $P_7$ – skewed cracking of a transverse reinforcing rib, $P_8(P_{8S})$ – radial cracking of the transverse rib (butt weld of the transverse rib), $P_{9S}$ – cracking of a fillet weld connecting the transverse ribs with the web of the peripheral rib, $P_{10S}$ – cracking of the fillet weld connecting the transverse ribs with the mantle.

Fast rate of fatigue crack formation and growth and the resulting need of frequent repairs greatly limit the safe usage and efficiency of hoisting installations. Having the above in mind, the authors undertook a task to assess the technical state of Koepe pulleys in hoisting installations by taking into account the fatigue problems. After the dynamic analysis of drive wheel structural elements, the fatigue strength analysis of the discussed wheel solutions was performed. The results were verified by the deformations measurements (stresses) in real objects under normal operational conditions obtained from a few Polish mines.

## 4. Strength analysis

A high intensity of fatigue failures found on the basis of flow detection tests for both types of pulleys indicates the unsatisfactory fatigue life in the considered period of their usage. In this situation, it became necessary to conduct a detailed strength analysis of the pulley construction, which would provide the foundations for the pulley modernisation, and thus allow for its further safe operation.

The aim of the undertaken strength analysis of Koepe pulleys in hoisting installations was obtaining complete information concerning the state of stresses occurring in the wheel components under the influence of usage stresses. Determining these stress states in the areas of the pulley construction subjected to extreme efforts, constituted the basis for assessing strength and durability (allowable period of operations). The obtained information concerning the values and distributions of stresses should allow to identify such areas in the Koepe pulley structures, which – due to the stress level – can be subjected to fatigue failures and should be periodically inspected by means of non-destructive testing.

On account of the above, the strength analysis of both types of drive wheels was done by performing the analysis of Koepe pulley construction using numerical methods. The finite element method (FEM) was applied [7] using computer programs 'FEMAP' and 'NE/Nastran', on the basis of the developed calculation models of the Koepe pulley structure, consisting of the adequate elements of the plate type and solid type that fully represented the geometry of the analysed structures [1–3].

### *4.1. Koepe pulley with U-shaped diaphragms*

Forces being the result of the influence of the hoisting ropes on the pulley (determined from Eqs. (2.1) and (2.3)) as well as the dead weight of the adequate structure elements constituted the loads for the basic numerical calculation model of the Koepe pulley structure ('MP').

The load, which originated from the forces in ropes, was adequately distributed along the contact line between the ropes and the wheel mantle. The assumed scheme of this load distribution along the rope-drum contact is presented in Fig. 4 [1].

This loading was estimated after taking into account the following parameters of the analysed hoisting installation:

- $\alpha_o = \varphi_{AC} = 203^\circ$ – angle of contact between the ropes and the Koepe pulley drum,
- $\mu = 0.25$ – coefficient of friction between the Koepe pulley lining and the ropes,

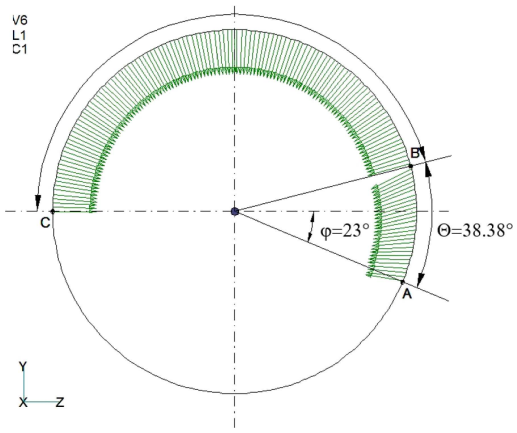


FIG. 4. The assumed scheme of the load distribution along the rope-drum contact [1].

- $\theta = \ln(S_1/S_2)/\mu$ – shear angle of the rope on the Koepe pulley,
- $p_\alpha = 2 \cdot S_\alpha/BD$ – the rope pressure on the Koepe pulley,
- $S_\alpha = S_2 \cdot e^{\mu \cdot \alpha}$ – the rope force as a function of the angle of contact,
- $t_\alpha = p_\alpha \cdot \mu$ – rope friction force on the Koepe pulley,

where $S_1$, $S_2$ – rope tensions on both sides of the Koepe pulley, $D$ – diameter of the Koepe pulley drum, $B$ – width of the rope contact surface with the Koepe pulley.

After introducing the proper equations and parameters, corresponding with the assumed load values, the applied computer program [1] automatically generated the values of forces and imposed them on the proper nodes of the finite elements network.

At the $A$-$B$ arch (Fig. 4) the load originated from the rope pressure and friction – changing its value in accordance with changing forces in the rope – was applied, while along the $B$-$C$ arch the load of a constant value originated from the rope pressing the mantle of the Koepe pulley drum.

The complete information on the deformation and stress states discussed in [2] for the skip hoist drum loaded with the maximum total force in ropes was obtained as a result of the performed computer simulations. The selected results of the computer calculations are presented in the form of contour plans, illustrating distributions of the reduced stress values $\sigma_H$, in accordance with the Huber-Mises hypothesis, in individual areas of the pulley model. The general view of the distribution of the reduced stress values $\sigma_H$ for the Koepe pulley (MP model), is shown in Fig. 5.

Performed calculations revealed that the most extreme stresses occurred in the places where the diaphragms were connected with the shaft hub (Fig. 5), i.e., in the areas where the fatigue cracks were most often observed.

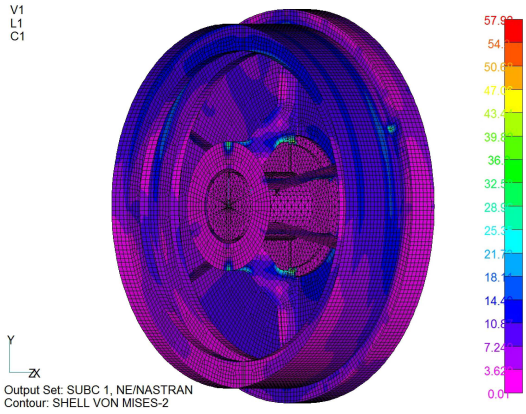


FIG. 5. Distribution of the reduced stress values $\sigma_H$ [MPa] for the Koepe pulley – MP model [1].

The analysis of the FEM results indicates that the components of the stress state – for the diaphragms – are periodically changing their values together with changing their placement, due to the pulley angular motion. Extreme values of main stresses ($\sigma_1$ and $\sigma_2$) are obtained when the diaphragm is situated in parallel to the resultant force in hoisting ropes, i.e., when it is in the plane of the maximum shaft deflection.

In order to determine the influence of length and geometry of the crack developing within the diaphragm on the stresses occurring in the pulley, the expanded FEM analysis based on the crack development mechanism – identified for this area – was carried out. This analysis was taking into account a successive crack length growth, which is illustrated in Fig. 6. Individual calculation mo-

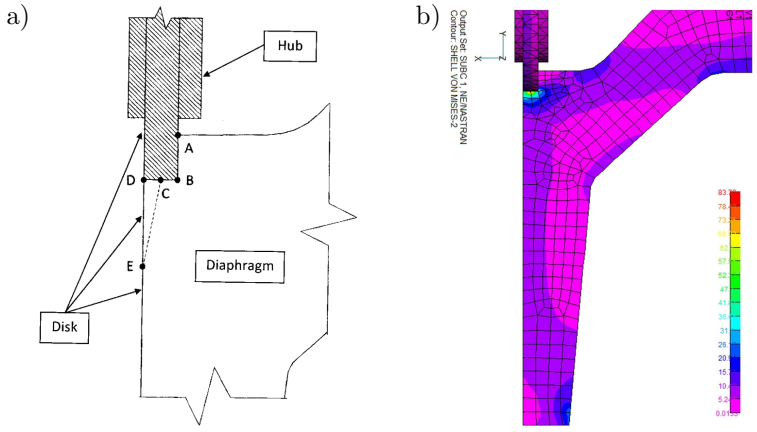


FIG. 6. a) Schematic presentation of the crack growth in the area connecting the diaphragm with the side disk, b) distribution of reduced stresses $\sigma_H$ [MPa] in the stretched diaphragm – model MB [1].

dels (M) corresponded to the successive stages of the crack length growth: MA – line *A-B*, MB – line *A-B-C-D*, MC – line *A-B-C-E*. Extreme values for main stresses $\sigma_1$, $\sigma_2$ and reduced stresses $\sigma_H$ in the diaphragms and the side disk, for all analysed models, are listed in Tables 1 and 2.

**Table 1**. List of extreme stress values in the diaphragm [2].

| Calculation model | Diaphragm placement: | | | | | |
|---|---|---|---|---|---|---|
| | above the shaft | | | below the shaft | | |
| | Stress values [MPa] | | | | | |
| | $\sigma_H$ | $\sigma_1$ | $\sigma_2$ | $\sigma_H$ | $\sigma_1$ | $\sigma_2$ |
| MP | 53.6 | −14.6 | −59.4 | 57.9 | 64.1 | 15.4 |
| MA | 48.9 | −19.9 | −54.1 | 51.3 | 56.4 | 18.9 |
| MB | 83.7 | −0.9 | −84.1 | 74.3 | 72.5 | 1.8 |
| MC | 43.7 | −19.3 | −49.8 | 47.7 | 53.8 | 19.3 |
| MK | 17.5 | −3.7 | −19.0 | 20.3 | 22.6 | 5.6 |

**Table 2**. List of extreme stress values in the disk [2].

| Calculation model | Diaphragm placement: | | | | | |
|---|---|---|---|---|---|---|
| | above the shaft | | | below the shaft | | |
| | Stress values [MPa] | | | | | |
| | $\sigma_H$ | $\sigma_1$ | $\sigma_2$ | $\sigma_H$ | $\sigma_1$ | $\sigma_2$ |
| MP | 8.1 | 3.6 | −6.5 | 9.6 | 7.3 | −5.1 |
| MA | 8.2 | 3.6 | −6.7 | 9.9 | 7.5 | −5.4 |
| MB | 39.8 | −8.2 | −43.0 | 38.9 | 40.8 | 4.6 |
| MC | 60.5 | −24.0 | −68.8 | 60.9 | 69.1 | 23.0 |
| MK | 16.1 | 3.6 | −14.0 | 18.1 | 15.2 | −4.7 |

The analysis of the FEM calculations indicates that the crack growth along line *A-B* (model MA) has no influence on the stress state and disk deformations. However, when the crack will grow to point *D* or *E*, i.e., when it will reach the side disk, its further growth will occur within the disk, causing failures illustrated in Fig. 2b.

The presented above calculation results indicate that the direct cause for the crack formation and growth is a significant over-rigidity of the pulley construction caused by the stiff diaphragms. The diaphragms locally limit the deformations of side disks caused by a shaft deflection, which is the reason for cyclic, alternate compressions and tensions of the diaphragms (in agreement with the Koepe pulley rotations). In consequence, this causes the formation of fatigue cracks in the high stress areas of diaphragms and side disks of the pulleys. This

fact is confirmed by the calculation results together with the results of strain gauge measurements [2, 8], shown in Table 3 for extensometers situated as shown in Fig. 7.

**Table 3**. List of strain gauges measurements and FEM calculations results [2].

| Measuring sensor number (Fig. 7) | Values of stress [MPa] obtained on the basis of: | | | | |
|---|---|---|---|---|---|
| | difference [%] | measurements | FEM calculations | | |
| | | $\sigma_p$ | $\sigma_H$ | $\sigma_1$ | $\sigma_2$ |
| P33 | −28.9 | 26.7 | 20.7 | 20.1 | −1.3 |
| P34 | 44.9 | 13.0 | 23.6 | 24.3 | – |
| P53 | 35.2 | 6.8 | 10.5 | 8.5 | 3.0 |
| PW | 46.6 | 10.1 | 18.9 | 18.4 | −0.2 |

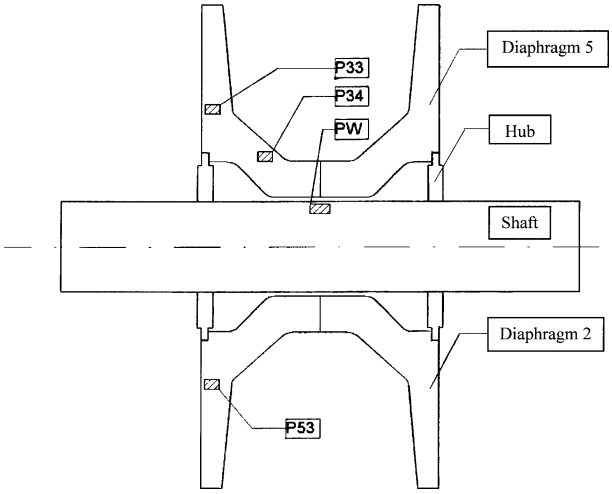


FIG. 7. Scheme of the placements of strain gauges on diaphragms and a shaft.

Significant differences in stress values obtained on the basis of FEM and measurements, shown in Table 3, reaching approximately 47% at measuring points P34 and PW, are probably caused by significant geometrical differences as compared with the design documentation that was assumed in calculations. These differences were caused – among others – in numerous local repairs and reinforcements performed using the welding process, which introduced additional welding stresses.

According to the requirements of mining regulations [9, 10], concerning the fatigue strength of welded joints (class D) made of S235 grade steel (of which the pulley was made), it can be assumed that this strength for the stretched butt weld is $R_w = 45$ MPa, while for the shear fillet weld: $R_w = 27$ MPa. The calculated stress values indicate that the reasons for fatigue failure formation and

growth in the Koepe pulley are exceedingly high fatigue strength values of the welded joints.

The analysis of the FEM results indicates that the removal of the middle part of diaphragms together with the ring joining them can have a beneficial influence on the state of stresses in the place of their connection with disks. Therefore, the additional calculation model 'MK' was prepared. In this model, the horizontal parts of diaphragms were removed, while their vertical parts connected with side disks remained. The distribution of reduced stresses in the diaphragms and in the side disk of the pulley, obtained for this model, is presented in Fig. 8 and in Tables 1 and 2.

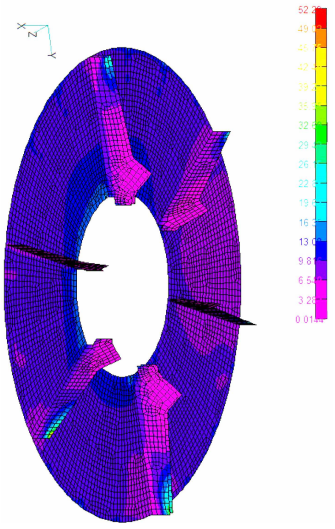

FIG. 8. Distribution of reduced stresses $\sigma_H$ [MPa] in diaphragms and disk of the MK model [1].

The results of calculations – listed in Tables 1 and 2 – indicate that removal of the horizontal parts of diaphragms significantly decreases the stress level within the areas of cracks formations, causing simultaneously approximately a two times increase of the stresses in side disks, the values of which still remain low. It should be mentioned that the removal of the middle part of diaphragms did not significantly change the drive shaft deflection.

### *4.2. Koepe pulley with two circumferential rings*

Forces being the result of hoisting rope influences on the Koepe pulley, determined from Eqs. (2.1) and (2.3) (taking dead weight into account), constituted loads for the numerical calculation model of the Koepe pulley with two circumferential rings. On account of finding that fatigue cracks occur in the wheel mantle area, three various stages of rope winding were considered: total rope

winding on the pulley, unwinding of one third of the coil and unwinding of half of the coil.

The distribution of reduced stresses $\sigma_H$ in the wheel mantle, for circumferential rings and transverse ribs – for the original solution from Fig. 3 – is presented in Fig. 9 [3]. The selected results of the FEM analyses for circumferential rings and transverse ribs for the original solution were compared with the results obtained for the modernised pulley. Three additional circumferential rings were adequately applied in place of the removed one. The results are presented as contour plans representing the distributions of reduced stress values $\sigma_H$, shown in Fig. 10 [3, 11].

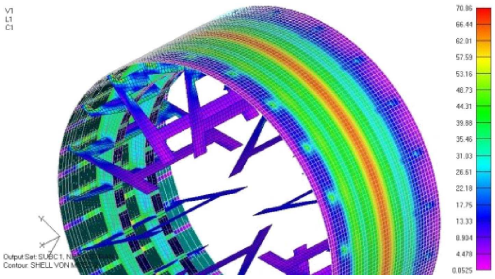

FIG. 9. Distribution of reduced stresses $\sigma_H$ [MPa] on the inner surface of the mantle – original structure, total winding of the rope [3].

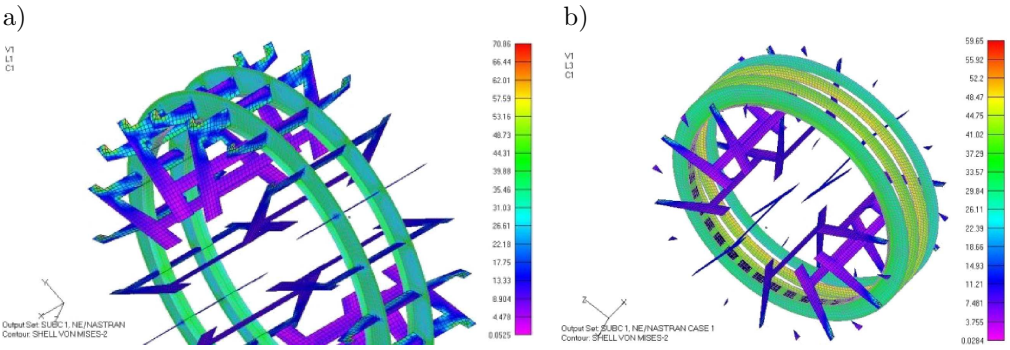


FIG. 10. Distribution of reduced stresses $\sigma_H$ [MPa] in rings and transverse ribs, for the total winding of the rope: a) original construction, b) modernised construction [3].

Computer simulations indicate that the highest stresses occur in the areas, in which the fatigue crack formation and growth were found. Thus, they explicitly indicate that the direct causes of fatigue cracks are unsatisfactory load-carrying capacity and stiffness of the pulley mantle.

In order to adequately increase the pulley mantle strength, several constructional solutions were considered [12]. Finally, the solution based on removal of

one of the rings strengthening the mantle (Fig. 10a) and substituting it with three other rings of smaller diameters, properly distributed, (Fig. 10b) was selected [3]. The selected results of the performed numerical analysis in form of diagrams showing stress changes along the mantle generating line are presented in Figs. 11 and 12.

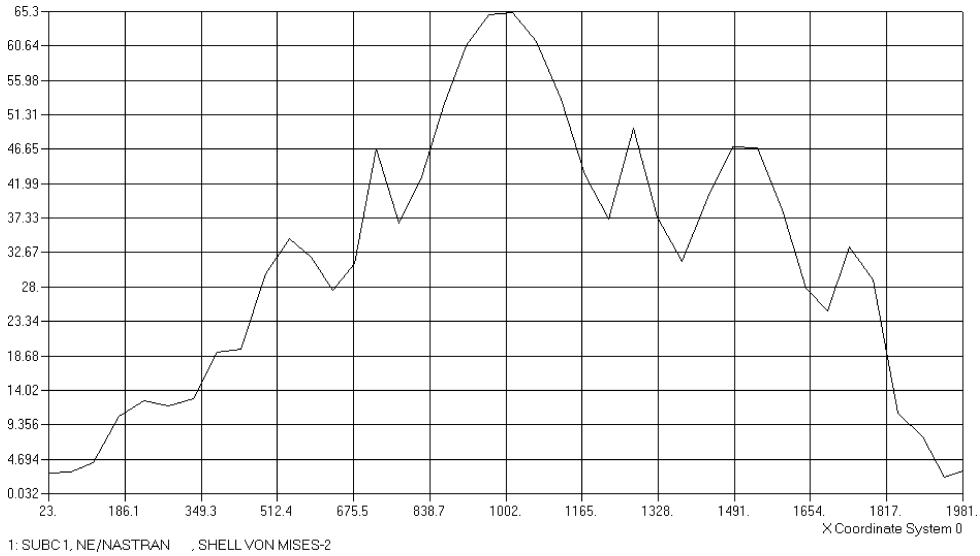


FIG. 11. Changes of the reduced stress values $\sigma_H$ [MPa] along the mantle generating line. Original solution – total rope winded on the pulley [3].

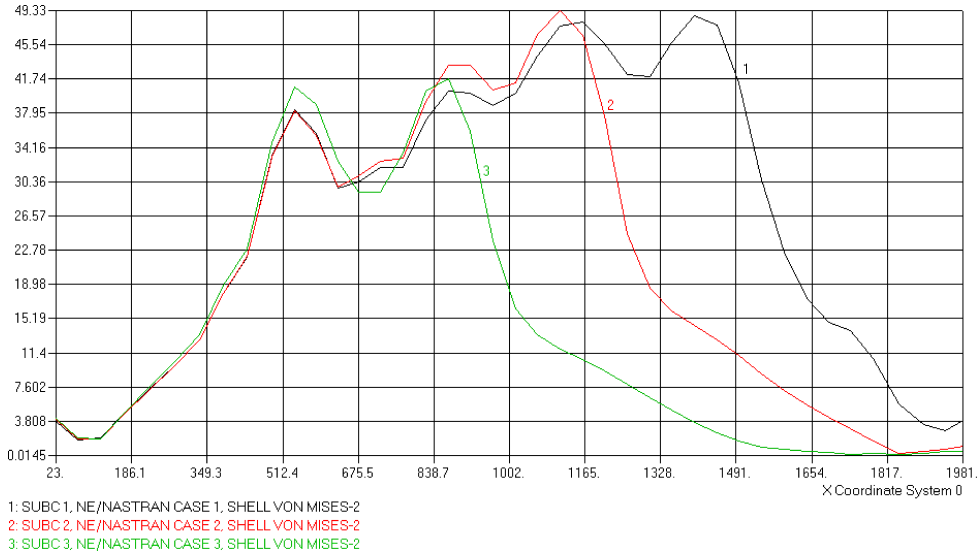


FIG. 12. Changes of the reduced stress values $\sigma_H$ [MPa] along the mantle generating line for three assumed load cases. Pulley after the reconstruction [3].

The selection of essential information on the values and distributions of deformations and stresses in calculation models was carried out on the basis of the numerical calculation results. For the modernised pulley construction, the radial displacements of the mantle decreased by 19%. Information concerning stress changes is given in Table 4.

**Table 4**. FEM results.

| Maximal reduced stress $\sigma_H$ [MPa] | Model | |
|---|---|---|
| | original design | re-design |
| In the model | 71 | 60 |
| On the mantle's external surface | 65 | 45 |
| On the mantle's internal surface | 55 | 49 |
| On the rings in contact with the mantle | 55 | 49 |
| On the rings' inside diameter | 43 | 46 |

Measurements of the operational stresses variability were performed with the application of the strain gauge method for the Koepe pulley operating in one of the Polish mines [3]. The scheme of strain gauge arrangement is shown in Fig. 13 [3]. The circumferential stresses in plates of stiffening rings were measured by strain gauges 1 and 2, while the circumferential and transverse stresses in two areas of the wheel mantle by gauges 3, 4, 5 and 6. Measurements were performed under the conditions of licensed work of the Koepe pulley, consisting of: skip hoist loading with allowable load at the loading station, ascending of the loaded skip (with full kinematic parameters), unloading at the unloading station, and descending of the empty skip (with full kinematic parameters).

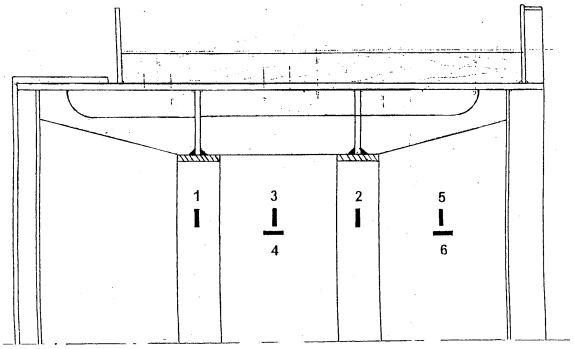


FIG. 13. Strain sensor arrangement on the drum.

The performed measurements indicated that for each work cycle of the pulley the circumferential stresses measured by extensometers 1, 2, 3 and 5 are compressible, while the transverse stresses measured by extensometers 4 and 6

are stretching. The values of stress ranges measured by individual extensometers are compiled in Table 5 together with the allowable stress rangesdetermined on the basis of the standard PN-B-03200:1990 [13], for the investigated wheel made of steel (S235 grade).

**Table 5**. Stress levels obtained by strain gauges measurements.

| Sensor | Stress range $\Delta\sigma$ [MPa] | | Admissible level exceeded by [%] |
|---|---|---|---|
| | measured | admissible | |
| 1 | 49 | 36 | 36 |
| 2 | 72 | 36 | 100 |
| 3 | 118 | 57 | 107 |
| 4 | 90 | 57 | 58 |
| 5 | 86 | 57 | 51 |
| 6 | 98 | 57 | 72 |

The results listed in Table 5 indicate that the stress values in all measuring points significantly exceed permissible values.

## 5. Final conclusions

Numerous fatigue cracks, mainly in the welded joints areas, were found in both discussed types of Koepe pulleys, one with U-shaped diaphragms and the second one with two circumferential rings stiffening the mantle, both being widely used in Polish mining for a long period of time, significantly exceeding 30 years.

The strength calculations of the pulleys performed on the basis of the performed dynamic analysis of hoisting installation, and verified by the strain gauge measurements of deformations on real objects, indicate that welded joints – applied in the considered constructions of Koepe pulleys – do not satisfy the requirements determined in the regulations [9, 10, 13], concerning the fatigue strength of category D welded joints made of S235 grade steel of which these wheels were made.

On the bases of the performed computer simulations (FEM) certain modifications of the drive wheels were proposed and realised for a few wheels operating in the Polish mines. Experiences collected after few years of their operations indicate a significant decrease in the number and intensity of fatigue cracks.

These strength calculations provided the basis for pointing out the construction areas of the considered pulleys subjected to the highest stresses as well as to determine the appropriate time for performing their non-destructive testing to prevent crack formation.

## Acknowledgment

This research was carried out as part of the statutory activity No. 11.11.130.375 of the Department of Strength and Fatigue of Materials and Structures, AGH UST in Cracow.

## References

1. Cichociński A., Ładecki B., Płachno M., Podsiadło A., Micek P., *The analysis of reasons of defects of the Koepe pulleys of hoisting installations 4L-3400/2400 type and documentations of their repairs* [in Polish], Work no 5.5.130.921, AGH University of Science and Technology, Faculty of Mechanical Engineering and Robotics, Kraków, 2002.
2. Cichociński A., Ładecki B., *Analysis of the causes of fatigue cracks in the construction of a motion wheel in hoisting machine* [in Polish], Mechanika, Wydawnictwa AGH, **24**(3): 166–172, 2005.
3. Cichociński A., Ładecki B., Płachno M., Podsiadło A., *Performing of analyses, measurements and development of repair works of the hoisting installation skip* [in Polish], Work No. 5.5.130.490, AGH University of Science and Technology, Faculty of Mechanical Engineering and Robotics, Kraków, 2005.
4. Wolny S., *Dynamic loading of the pulley block in a hosting installation in normal operating conditions*, Archives of Mining, **54**(2): 261–284, 2009.
5. Wolny S. Płachno M., *Experimental verification of bearing rope loading in typical operating conditions of the hoisting installation*, Archives of Mining Science, **54**(3): 531–542, 2009.
6. Wolny S., Badura S., *Stress analysis in structural components of the Koepe pulley in hoisting installations*, Engineering Transactions, **62**(2): 155–170, 2012.
7. Zienkiewicz O.C., Taylor R.L., *Finite Element Method* (5th Ed.), Butterworth-Heinemann, Oxford and Boston, 2000.
8. Hoffmann K., *An Introduction to measurements using strain gages*, Hottinger Baldwin Messtechnik GmbH, 1989.
9. *Technical conditions of designing, performing and acceptance of welded joints in mining objects, devices and machines* [in Polish], Biuro Studiów i Projektów Górniczych, Katowice, 1982.
10. *Appendix No. 17 to the Regulation of the Minister of Industry and Trade, Vol. IV (Shaft Hoist). Requirements concerning building and maintenance of mining shaft hoists* [in Polish], Wyd. „KADRA", Katowice, 1995.
11. Wolny S., Ładecki B., *Assessment of stress state of the supporting elements of the pulley block in a hoist installation.* Transport Przemysłowy i Maszyny Robocze, **4**(22): 67–71, 2013.
12. Henry F.D.C., *The Design and Construction of Engineering Foundations*, Chapman and Hall, Norwell, Massachusetts, USA, 1986.
13. PN-90/B-03200. *Steel structures. Design rules*, Polish Standard, Warsaw, 1990.

*Received August 11, 2016; accepted version June 9, 2017.*